



Conventional MRI features of adult diffuse glioma molecular subtypes: a systematic review

Arian Lasocki^{1,2} · Mustafa Anjari³ · Suna Örs Kokurcan^{3,4} · Stefanie C. Thust^{3,5}

Received: 1 June 2020 / Accepted: 17 August 2020
© Springer-Verlag GmbH Germany, part of Springer Nature 2020

Abstract

Purpose Molecular parameters have become integral to glioma diagnosis. Much of radiogenomics research has focused on the use of advanced MRI techniques, but conventional MRI sequences remain the mainstay of clinical assessments. The aim of this research was to synthesize the current published data on the accuracy of standard clinical MRI for diffuse glioma genotyping, specifically targeting IDH and 1p19q status.

Methods A systematic search was performed in September 2019 using PubMed and the Cochrane Library, identifying studies on the diagnostic value of T1 pre-/post-contrast, T2, FLAIR, T2*/SWI and/or 3-directional diffusion-weighted imaging sequences for the prediction of IDH and/or 1p19q status in WHO grade II-IV diffuse astrocytic and oligodendroglial tumours as defined in the WHO 2016 Classification of CNS Tumours.

Results Forty-four studies including a total of 5286 patients fulfilled the inclusion criteria. Correlations between key glioma molecular markers, namely IDH and 1p19q, and distinctive MRI findings have been established, including tumour location, signal composition (including the T2-FLAIR mismatch sign) and apparent diffusion coefficient values.

Conclusion Consistent trends have emerged indicating that conventional MRI is valuable for glioma genotyping, particularly in presumed lower grade glioma. However, due to limited interobserver testing, the reproducibility of qualitatively assessed visual features remains an area of uncertainty.

Keywords Glioma · Glioblastoma · Magnetic resonance imaging · Radiogenomics · Imaging genomics

Electronic supplementary material The online version of this article (<https://doi.org/10.1007/s00234-020-02532-7>) contains supplementary material, which is available to authorized users.

✉ Arian Lasocki
arian.lasocki@petermac.org

- ¹ Department of Cancer Imaging, Peter MacCallum Cancer Centre, Grattan St, Melbourne, Victoria 3000, Australia
- ² Sir Peter MacCallum Department of Oncology, The University of Melbourne, Parkville, Australia
- ³ Lysholm Department of Neuroradiology, National Hospital for Neurology and Neurosurgery, London, UK
- ⁴ Department of Diagnostic Neuroradiology, Health Science University, Bakirkoy Dr Sadi Konuk Training and Research Hospital, Istanbul, Turkey
- ⁵ Department of Brain Repair and Rehabilitation, Neuroradiological Academic Unit, UCL Institute of Neurology, London, UK

Introduction

Diffuse astrocytic and oligodendroglial brain tumours occur along a continuum from World Health Organization (WHO) grade II (diffuse astrocytoma and oligodendroglioma) and grade III (anaplastic astrocytoma and anaplastic oligodendroglioma) to grade IV (glioblastoma, GBM) [1]. The latest 2016 WHO update to the Classification of Tumours of the Central Nervous System has acknowledged the prognostic importance of molecular parameters, which now constitute a key component of glioma diagnosis, providing an integrated phenotypic and genotypic diagnosis [1]. This has generated a new clinical need for correlating imaging features with glioma genotypes, known as radiogenomics or imaging genomics.

In the current (2016) WHO classification, grade II and III gliomas are considered together (lower grade gliomas, LGG), but distinct from GBM [1]. Irrespective of grade, the first step in glioma molecular characterisation is isocitrate dehydrogenase (IDH) testing [1]. Most LGG (> 70%) harbour an IDH

mutation (IDH-mutant, IDH^{mut}), which is associated with significantly longer survival [2]. For IDH^{mut} LGG, 1p19q genotyping follows to distinguish between tumours with 1p19q codeletion (molecular oligodendrogliomas, demonstrating combined loss of both the short arm of chromosome 1 and long arm of chromosome 19, IDH^{mut}/1p19q^{codelet}) and those without (molecular astrocytoma, IDH^{mut}/1p19q^{intact}) [1]. In contrast, LGG without an IDH mutation are known as IDH-wildtype (IDH^{wt}), and can be considered “molecular GBM” if also associated with other characteristic mutations [3, 4]. For tumours with histological evidence of GBM, IDH testing suffices [1]. IDH^{mut} GBMs are rare (< 10% of all GBMs) [2] and hypothesised to arise from LGG, with correspondingly better outcomes than IDH^{wt} [2].

This molecular characterisation gives rise to 3 prognostically relevant groups for imaging research in glioma: IDH status of LGG; 1p19q status of LGG; and IDH status of GBMs. Radiogenomics studies have primarily focused on the use of advanced MRI techniques for genotyping, including perfusion, spectroscopy and computational algorithms. However, specialist neuro-oncology centres receive referrals, and thus imaging, from a variety of outside institutions, which often utilize less comprehensive protocols. Repeating imaging and/or performing additional advanced sequences pending tissue diagnosis is often impractical, and while such a practice is valuable from a research perspective, it may not necessarily change management. As a result, anatomical MRI sequences remain the basis of the pre-operative MRI characterisation. In addition, the methodology around advanced techniques – both in acquisition and post-processing – is variable, limiting reproducibility and clinical translation. Computational imaging approaches such as machine learning offer new opportunities for the recognition of microstructural tissue patterns, but most have not undergone in-depth clinical testing. Specifically, there is a risk of “over-fitting” when training with a fixed set of imaging parameters in research, with accuracy decreasing when encountering the more variable clinical environment. In this context, human observers may more flexibly recognize morphological differences without a substantial detriment to accuracy.

It remains uncertain to what extent assessments in routine clinical practice can predict glioma genotypes. What can be considered “conventional” in MRI has evolved over time, but is largely based around anatomical sequences. Ellingson et al. have outlined a consensus brain tumour protocol for clinical trials, which consists of axial T2-weighted imaging (T2WI), axial (or volumetric) FLAIR (fluid attenuated inversion recovery), axial DWI (diffusion-weighted imaging) and pre- and post-contrast volumetric T1-weighted imaging (T1WI) [5]. DWI and susceptibility-sensitive sequences such as T2* and susceptibility-weighted imaging (SWI) are routinely performed in many institutions [6], and may nowadays also be considered part of basic MRI protocols.

To date, a limited number of reviews have summarized conventional imaging features of glioma molecular subtypes [7], whereas the bulk of literature on this topic was published in recent years and is constantly evolving. The aim of this research was to systematically review and synthesize currently available data on the accuracy of standard clinical MRI for diffuse glioma genotyping. For the purpose of this study, we have considered sequences as “conventional” in line with recently published guidance on glioma imaging [5, 6], on the proviso that the results description was not solely based on advanced analytic techniques (e.g. computational learning).

Methods

This research was carried out according to the Preferred Reporting Items for Systematic Reviews and Meta-Analyses (PRISMA-DTA) criteria [8]. The study has been registered in the PROSPERO online database of systematic reviews (CRD42019127655).

Data sources

A systematic search was performed in September 2019 using PubMed and the Cochrane Library (until September 2019). The following search key words were used: (“brain tumo(u)r”, “glioma”, “glioblastoma”, “astrocytoma”, “oligodendroglioma”) AND (“isocitrate dehydrogenase”, “IDH”, “1p19q”, “1p/19q”, “molecular”, “WHO 2016”) AND (“magnetic resonance imaging”). Further details of the search strategy are shown in Supplementary Material 1.

Study selection

The abstracts of all articles retrieved in the initial search were screened independently by two reviewers (board-certified radiologists with research experience in neuro-oncology). All selected full-text manuscripts were reviewed independently by two reviewers (from a team of four board-certified reviewers), with abstracts chronologically randomized and reviewer pairings varied to avoid bias. A stepwise selection was performed independently by each reviewer according to the same method. The exclusion criteria were: no interpretation of conventional MRI sequences (defined as T1 pre-/post-contrast, T2, FLAIR, T2*/SWI and/or 3-directional DWI [6]); animal/laboratory measurements only; technical comparison between different MRI acquisition technique(s); studies confined to physiological MRI (e.g. perfusion, spectroscopy, diffusion tensor or kurtosis imaging, functional imaging methods) or machine learning; studies restricted to predicting WHO histological grade; studies lacking glioma molecular subtype information; studies reporting on prognosis only; review articles; case reports of < 5 cases; studies only examining

molecular markers other than IDH and 1p19q; conference abstracts; or no English full text. The inclusion criteria were: studies examining the diagnostic value of MRI regarding IDH and/or 1p19q in the context of WHO grade II-IV gliomas; assessment of conventional MRI sequences (as defined above) performed on glioma patients pre-treatment; and description of qualitative and/or quantitative glioma feature(s). In cases of disagreement, each full-text article was reviewed and the discrepancy resolved in consensus with a third (senior) reviewer. A summary of inclusions and exclusions is provided in Fig. 1.

Data analysis

The results of the included studies were documented with the use of a data extraction form to derive the glioma molecular information tested, diagnostic MRI sequence(s) used, descriptive and statistical results, and method characteristics. The latter included study design and institute of origin, number of patients, participant age, tumour histology and molecular data, MRI field strength, contrast agent, feature description,

quantification (e.g. region of interest (ROI) placements) and interobserver testing. Each of the reviewers independently performed the full-text screening followed by the data extraction with two reviewers analysing each publication. Discrepancies were resolved in consensus with a third reviewer. A summary of the data extraction table is presented in Supplementary Material 2.

Study quality assessment

The study quality was examined using the Quality Assessment of Diagnostic Accuracy Studies (QUADAS-2) instrument [9]. We evaluated concerns regarding applicability in three domains (low, high, unclear) and the risk of bias in four different domains (patient selection, index test, reference test, timing). Each study was independently assessed for quality and potential bias by two reviewers. Disagreements were resolved by consensus with a senior reviewer.

Statistical analysis

Descriptive data are presented in the form of a narrative synthesis, because of the perceived heterogeneity of reported imaging features, assessment methods and lack of consistent quantification.

Data synthesis

Results overview

Forty-four studies including a total of 5286 patients fulfilled the inclusion criteria, with a mean of 115.9 (standard deviation 73.1) gliomas analysed in each study. Of these, 30 studies were confined to LGG analysis: 3 studies assessed WHO grade II tumours, 6 evaluated WHO grade III and 21 studies included WHO grades II and III. Grade IV tumours were examined in 8 studies. Five studies assessed WHO grade II-IV gliomas, while one further study included WHO grades I-IV. 18 studies examined IDH alone, 6 1p19q alone, and 20 studies assessed both. 7 studies identified only investigated molecular markers other than IDH and 1p19q, and were thus excluded from further analysis.

All included studies were retrospective analyses. Twelve studies reported statistical results (κ) for interobserver comparisons of qualitative features, 2 studies reported intraclass correlation coefficient (ICC) values for quantitative glioma properties, 13/44 studies performed consensus reads using ≥ 2 observers, and 24 publications used either a single reader (7/44) or lacked comprehensive information on reader methods (12/44).

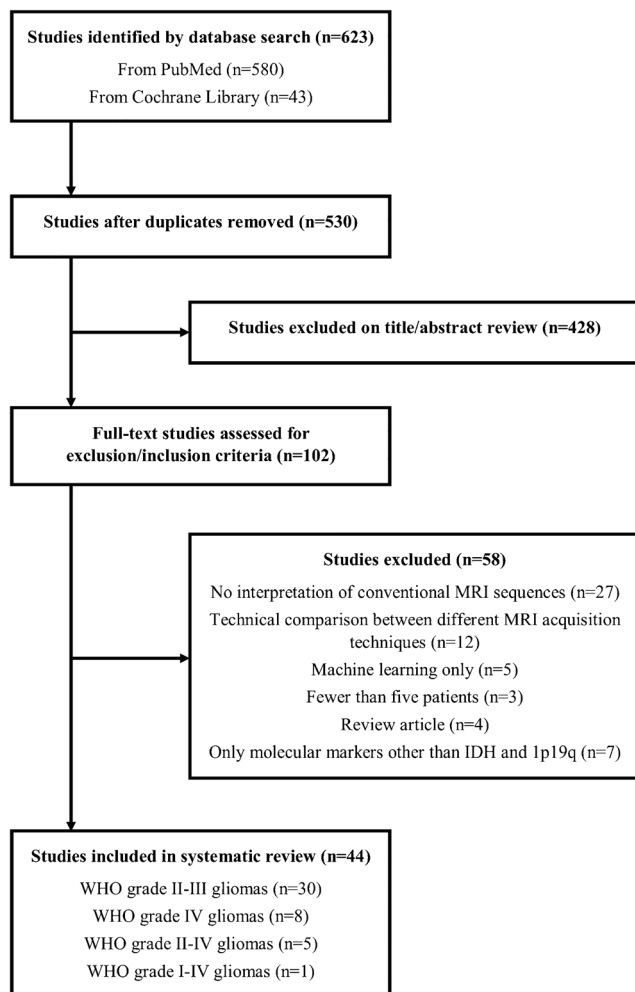


Fig. 1 CONSORT diagram of the study selection process

WHO grade II/III glioma (LGG) genotyping

IDH

Tumour location Sixteen studies assessed the relationship between tumour location and IDH status in LGG. A predilection of IDH^{mut} tumours to occur in the frontal lobes was identified by multiple research groups [10–17]. Most of these studies showed statistical significance, but only one study provided sensitivity (72.2%) and specificity (63.3%) [12]. A smaller number of studies reported correlations between IDH^{wt} status and other locations, specifically thalamus (11/52 IDH^{wt} compared with 0/68 IDH^{mut}; $p = 0.001$) [15] and brainstem (all brainstem tumours in one cohort were reportedly IDH^{wt}, without subgroup numbers provided) [18]. Sonoda et al. observed that anaplastic gliomas sparing the cerebral cortex were more likely IDH^{wt} (13/44 IDH^{wt}, 0/78 IDH^{mut}; $p < 0.0001$) [11]. In a study by Kanazawa et al, non-temporal location was the sole imaging feature that was significantly associated with IDH status, with limited specificity (57.1%) [19]. High interobserver agreements were reported for laterality ($\kappa = 1.00$) and location ($\kappa = 0.723$ – 1.00) [15, 20].

A study of 193 patients by Qi et al. found that IDH^{mut} tumours more commonly involved a single lobe, whereas IDH^{wt} tumours were predominantly located in combined lobes such as the diencephalon or brainstem ($p < 0.001$) [10]. Park et al. reported that a “nonlobar location” was associated with IDH^{wt} genotype (adjusted odds ratio (OR) 2.38), though a definition of “nonlobar location” was not provided [20]. Multifocality, multicentricity or a gliomatosis cerebri pattern have been identified as predictive of IDH^{wt} status in two further, relatively large study samples ($n = 146$ and $n = 175$, respectively) [15, 20]. Contrary to these findings, IDH^{mut} LGG may be larger than IDH^{wt} tumours at diagnosis [13, 21].

Internal signal characteristics and gadolinium enhancement

Multiple studies have examined signal characteristics of LGG. IDH^{mut} LGG were more commonly homogeneous in one cohort (79% of 89 IDH^{mut}, compared with 45% of 104 IDH^{wt}) [10], while cystic change appears less frequent in IDH^{wt} tumours [18, 22]. Enhancement is more common in IDH^{wt} tumours: Wu et al. found enhancement in 93% of IDH^{wt} tumours compared with 57% IDH^{mut} [22], and similar results were reported in the cohort of anaplastic gliomas examined by Wang et al. (88% IDH^{wt} and 68% IDH^{mut}) [23]. Providing further support, Juratli et al. found that enhancing gliomas were more common in IDH^{wt} tumours (57%) than both IDH^{mut}/ATRX-inactivated and IDH^{mut}/1p19q^{code1} tumours (28% and 25%, respectively) [24]. IDH^{wt} tumours have also been associated with a greater degree of enhancement [10, 16, 20, 22, 25]. Ring-enhancement of LGG (i.e. MRI evidence of necrosis) correlated with IDH^{wt} status in several studies [11, 22, 26]. In a logistic regression model utilizing Visually

AcceSable Rembrandt Images (VASARI) features [27], the proportion of enhancing lesion necrosis was one of two optimal features (together with tumour size), which moderately predicted IDH status of LGG (area under the curve, AUC 0.73) [28]. Similar to these findings, a different study examining VASARI features identified the proportion of the tumour that was non-enhancing as the single best feature for predicting an IDH mutation, with high accuracy (AUC 0.92) [25].

Tumour margins Sharp tumour margins have been associated with LGG IDH^{mut} status [10, 13], while poor definition of the non-enhancing margin has been correlated with IDH^{wt} status in multiple publications [15, 17, 20]. Of these, only one study, by Park et al, reported interobserver agreement ($\kappa = 0.766$) [20]. One study identified that a lower T1/FLAIR ratio was more frequent in IDH^{wt} gliomas, together with deep white matter invasion, but interobserver agreement was not specifically reported [15]. One study, in which two readers assessed VASARI features in consensus, suggested that oedema was more common in IDH^{wt} LGG [22].

Diffusion-weighted imaging A variety of ADC metrics have been examined, with higher ADC values consistently reported in IDH^{mut} LGG compared with IDH^{wt}. Villaneuva-Meyer et al. observed that ROI-derived minimum, mean and maximum ADC correlated with IDH status; of these, a minimum ADC threshold of 0.9×10^{-3} mm²/s provided the greatest sensitivity (91%) and specificity (76%), with an AUC of 0.901 [18]. Wasserman et al. performed ROI-based minimum ADC assessments and reported a significant association with IDH genotype, with an optimal cutoff point of 0.95×10^{-3} mm²/sec (sensitivity 76.9%, specificity 65.2% and AUC 0.711) [12]. Xing et al. investigated minimum ADC and relative minimum ADC (comparing to contralateral normal-appearing white matter) based on multiple ROIs placed in each glioma, with both yielding statistically significant results; the reported optimal minimum ADC threshold was 1.01×10^{-3} mm²/sec (sensitivity 76.9%, specificity 82.6%; AUC 0.87) [14]. Liu et al. assessed both mean and minimum ADC; results for mean ADC reached statistical significance ($p = 0.028$), while those for minimum ADC did not ($p = 0.069$) [29]. However, there were only 15 WHO grade II/III gliomas in this cohort, and AUC analysis was not presented [29]. Thust et al. assessed single-slice mean ADC normalized to the contralateral centrum semiovale normal-appearing white matter in 44 non-enhancing LGG, achieving AUC of 0.95 for one reader (optimal ADC_{ratio} cutoff 1.83) and AUC of 0.96 (optimal ADC_{ratio} cutoff 1.76) for the other reader [30]. Notably, single-slice ADC measurements correlated strongly with whole lesion assessment in this study [30]. Of these 5 studies, 2 reported ICC results of 0.71–0.91 [18] and 0.98 [30] for ROI-derived ADC values.

1p19q

Tumour location A frontal lobe location has repeatedly been associated with 1p19q codeletion [13, 26, 31–33]. As a potential confounder, some of these studies may have included IDH^{wt} tumours amongst “non-codeleted” gliomas [26, 32, 33]. In the studies specifically comparing IDH^{mut}/1p19q^{codelet} and IDH^{mut}/1p19q^{intact} tumours, the results are heterogeneous and the lobar association is less compelling. Batchala et al. nevertheless reported a significant association between a frontal lobe location and codeletion in 102 IDH^{mut} LGG (OR 5.68, 95% CI 2.08–15.44; $p = 0.001$) [31]. In contrast, Sonoda found no significant difference in the frequency of a frontal lobe location between the 1p19q^{codelet} (74%) and 1p19q^{intact} tumours (67%; $p = 0.61$) [11]. The lobar distribution was also similar in the cohort of Darlix et al. (frontal location in 45% of 1p19q^{codelet} and 42% of 1p19q^{intact}) [13]. Several studies observed that a temporal lobe location reduces the likelihood of 1p19q^{codelet} genotype ($p = 0.011$ – 0.034) [11, 19, 32, 34], with one reporting no case of temporal-centred 1p19q^{codelet} in a cohort of 123 anaplastic gliomas [11]. Sherman et al. found that 1p19q^{codelet} tumours were more commonly confined to a single lobe than non-codeleted tumours [34]. The data on 1p19q genotype and cortical involvement are ambiguous, with one study demonstrating a statistical association with codeletion ($p = 0.02$) [16], and another showing no significant association [33]. One study reported weak interobserver correlation (42%) for cortical involvement [35].

Internal signal characteristics and gadolinium enhancement

As for IDH, internal signal characteristics have been examined by multiple authors. Yamauchi et al. identified that heterogeneous T2 signal was significantly more common in 1p19q^{codelet} tumours (94%) than both 1p19q^{intact} (33%) and IDH^{wt} tumours (50%), using consensus assessments [16]. Three further studies observed that tumour heterogeneity correlated significantly with 1p19q codeletion, but this feature did not permit a reliable IDH genotype distinction [19, 26, 33]. Batchala et al. observed that LGG which were < 75% homogeneous were much more likely to be 1p19q^{codelet} than 1p19q^{intact} ($p < 0.001$), with an OR of 12.33 and $\kappa = 0.69$ [31]. Similarly, Johnson et al. found that, while it was overall uncommon for a tumour to be completely homogeneous, homogeneity was more frequent in 1p19q^{intact} LGG (14% and 10% based on T1- and T2-weighted imaging, respectively) than in codeleted gliomas (1%), also by consensus assessment [32].

1p19q codeleted tumours have shown a correlation with either absent or ill-defined enhancement [16, 26, 36], in contrast to more nodular or ring-like enhancement in 1p19q^{intact} LGG [36]. One group reported that 1p19q^{codelet} tumours more commonly demonstrated $\leq 5\%$ enhancing tumour [37]. In contrast, a different study assessing anaplastic gliomas concluded that 1p19q^{codelet} tumours more commonly enhance than non-

codeleted tumours, but this was assessed in a binary fashion, with no distinction made between different qualities of enhancement [11].

Tumour margins Several studies have assessed tumour margins, most utilizing a binary distinction. Kim et al. found that an indistinct rather than sharp border correlated with 1p19q codeletion on both T1- and T2-weighted imaging ($p = 0.005$ and $p = 0.036$, respectively) [33]. Similarly, Johnson et al. observed that the majority of 1p19q codeleted tumours lacked sharp borders on both T1- and T2-weighted images (97% for each), with $p < 0.0001$ for each marker of border sharpness evaluated, and an odds ratio of 16.35 [32]. Conversely, a sharp border was much more common in non-codeleted tumours, with an incidence of 40% and 38% based on T1- and T2-weighted imaging, respectively [32]. Kanazawa et al. reported a strong correlation ($p = 0.002$), though only assessed tumour borders on T1WI [19]. Some studies have not shown a significant difference [16, 22]. Darlix et al. described tumour borders as sharp, indistinct or intermediate, and found that 1p19q^{codelet} tumours more commonly had intermediate borders, while indistinct tumour borders were more frequent in IDH^{wt} tumours [13]. No studies reported interobserver statistics for 1p19q tumour border evaluations.

Calcifications, haemorrhage and magnetic susceptibility

Several studies have examined associations with calcifications and haemorrhage, but there is substantial variability in the literature in how these are assessed, both regarding whether CT has been performed and with respect to MRI techniques. Calcification has been shown to predict 1p19q codeletion [16, 19, 35]. In one of these studies, paramagnetic susceptibility on T1WI (T1 shortening) was examined and this too was associated with codeletion, but not as strongly [19]. T2* blooming also predicted codeletion in one study [31]. Other studies which used MRI to assess for calcification [33] and paramagnetic susceptibility artefact [32] did not show a difference, but did not pursue a distinction of calcification from blood products based on the phase. Indeed, one study examining MRI suggests that haemorrhage is associated with codeletion, but did not evaluate calcification or discuss how these characteristics were separated [37]. All studies consisted of consensus reads, except one, which reported a moderate interrater agreement for T2* blooming, with $\kappa = 0.74$ [31].

T2-FLAIR mismatch The T2-FLAIR mismatch sign has been examined by several authors since being first described in 2017 [38]. Three studies concluded that the presence of T2-FLAIR mismatch is 100% specific for an IDH^{mut}/1p19q^{intact} tumour, with interobserver agreements between 0.56 and 0.75 [31, 38, 39]. Another study also found that all patients with > 50% T2-FLAIR mismatch were 1p19q^{intact}, though definitive IDH testing results were not available for patients with

negative IDH1-R132H immunohistochemistry [35]. In contrast, Juratli et al. had a false-positive rate of 28.5% for T2-FLAIR mismatch [24]. This study included enhancing gliomas, and separate results for non-enhancing gliomas in this cohort were not provided [24]. All false-positive cases were 1p19q^{code1}, with no false-positive IDH^{wt} cases reported [24].

Diffusion-weighted imaging With the caveat that a minority of IDH^{wt} tumours (which are associated with lower ADC values as summarized above) may have been included in some of the studies assessing DWI, 1p19q codeletion has consistently been associated with lower mean ADC values compared with IDH^{mut}/1p19q^{intact} LGG ($p = 0.0005$ – 0.003) [30, 32, 40], with two studies suggesting an ADC mean cutoff in the region of 1.4 – 1.6×10^{-3} mm²/s for 1p19q genotyping [32, 40].

Glioblastoma

IDH

Tumour location Publications on the geographical distribution of IDH genotypes in GBM broadly correspond to descriptions in LGG, supportive of a continuum of disease. Carrillo et al. found that 11 of 14 (79%) IDH^{mut} GBMs (comprising 7% of all GBMs in their cohort) were located in the frontal lobes, compared with only 69 of 188 (37%) IDH^{wt} [41]. Xing et al. also identified a geographic correlation with IDH status ($p = 0.002$), with 9 of 10 (90%) IDH^{mut} GBMs being located in the frontal lobes, compared with 23 of 60 (38%) IDH^{wt} [42]. The cohort of Lasocki et al. displayed a similar frequency of frontal lobe location in both IDH^{wt} (38%) and IDH^{mut} (40%) GBMs, but there were only 5 IDH^{mut} GBMs in this study [43]. In contrast, the IDH^{mut} GBMs in the cohort of Hong et al. displayed a higher frequency of an insular location than IDH^{wt} (33% compared with 12%; $p = 0.01$) [44], and Hata et al. reported that all five IDH^{mut} tumours in their cohort of 92 GBMs involved the insula [45].

Enhancement and noncontrast-enhancing tumour In a study by Yamashita et al, the necrotic area inside the largest cross-sectional enhancing lesion and the largest cross-section necrosis percentage were both associated with IDH status ($p < 0.005$) [46]. Wang et al. found that IDH^{mut} GBMs were slightly less likely to demonstrate enhancement (73.3%, compared with 94.9% for IDH^{wt}; $p < 0.001$) [47]. When the tumour did enhance, multiple enhancing foci were more common in IDH^{mut} tumours (42.4%, compared with 19.3% for IDH^{wt}; $p = 0.003$), though the distribution of contrast enhancement patterns did not differ significantly between IDH^{mut} and IDH^{wt} GBMs [47]. The presence of enhancing satellites positively correlated with IDH mutations in another cohort [41].

Similar to these findings, a larger proportion of noncontrast-enhancing tumour (nCET) has been associated

with IDH mutations. All 14 IDH^{mut} GBMs in the cohort of Carrillo demonstrated nCET, and a higher percentage of nCET was shown to correlate with IDH^{mut} status; the proportion of IDH^{wt} tumours with nCET was not specified, however [41]. Hong et al. identified a larger T2WI tumour volume in IDH^{mut} GBMs and a higher volume ratio between T2WI and contrast-enhanced T1WI in IDH^{mut} GBMs ($p < 0.05$) [44]. Similarly, in a study by Lasocki et al, 60% of IDH^{mut} GBMs had > 33% nCET, compared with 21% of IDH^{wt}, though this did not reach statistical significance ($p = 0.073$) [43]. This study highlighted that nCET was also common in IDH^{wt} tumours, with 57% of IDH^{wt} GBMs containing $\geq 5\%$ nCET [43]. To overcome this limited specificity, the same group subsequently proposed that a mass-like morphology of nCET could potentially provide better specificity for the prediction of an IDH mutation than the presence of nCET alone [48]. A larger GBM size at diagnosis and the presence of cysts have also been associated with IDH mutations [41].

Diffusion-weighted imaging In a study of 176 patients by Hong et al, IDH^{mut} GBMs demonstrated higher mean normalized ADC (2 reader ICC 0.97) in both T2-hyperintense non-enhancing (1.64×10^{-3} mm²/s for IDH^{mut}, 1.49×10^{-3} mm²/s IDH^{wt}; $p = 0.022$; sensitivity 66.7% and specificity 65.2% for ADC > 1.57×10^{-3} mm²/s) and enhancing areas (1.80 IDH^{mut}, 1.54 IDH^{wt}; $p = 0.008$; sensitivity 77.8% and specificity 53.8% for ADC > 1.53×10^{-3} mm²/s) [44]. Another study ($n = 75$) by Xing et al. found IDH^{mut} GBMs to have higher relative minimum ADC values in the enhancing region (AUC 0.703) [42].

Study quality

The results of the study quality assessment using the QUADAS-2 tool [9] are summarized in Fig. 2, with additional information available in Supplementary Material 3. Several

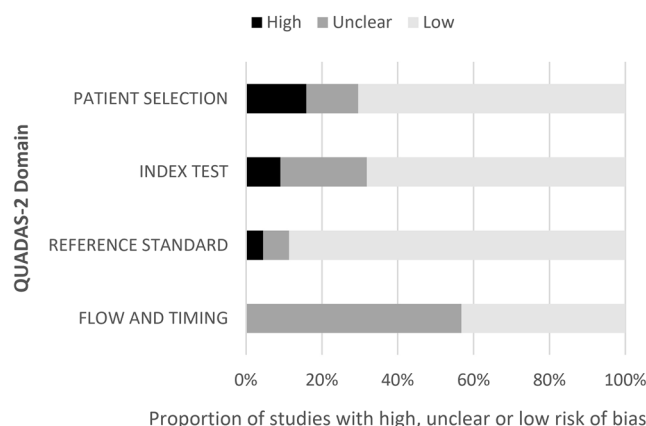


Fig. 2 Results of the QUADAS-2 quality assessment of the included studies. The risk of bias in four different domains is shown

(7/44) studies had a high risk of bias regarding patient selection. In addition, 7/44 studies were unclear about the selection of patients and/or the conduct or interpretation (5/44) of the index test. All research was of retrospective design. 23% (10/44) of studies lacked information on whether index test results were interpreted without knowledge of the reference standard, while 23% of studies gave insufficient information on whether reference standards were defined without knowledge of index test results.

Discussion

This systematic review aimed to summarize and appraise the literature on conventional MRI for glioma radiogenomic predictions. Due to a wide variation in the assessment and reporting methods, we did not proceed to a statistical (meta-analysis) evaluation for any particular sequence or imaging biomarker(s). To group studies with similar topic themes, the LGG and GBM data were presented in separate sections; however, the key results support that molecular-specific imaging features occur on a continuous spectrum across grades. For this reason, the following discussion is structured according to morphology.

Location (by epicentre) appears to be a valuable, static and reproducible tumour property with some of the highest interobserver ratings (κ) achieved in single centre studies [15, 20] and in multi-rater, multi-timepoint testing (VASARI criteria (laterality $\kappa = 0.943$, 95% CI 0.915–0.982 and tumour location $\kappa = 0.837$, 95% CI 0.807–0.902)) [27]. A frontal lobe location suggests an IDH mutation [10–16], with 1p19q^{code1} marginally favoured over 1p19q^{intact} [13, 31]. In contrast, an IDH^{mut} tumour located in a temporal lobe is unlikely to be 1p19q^{code1} [11, 19, 32]. In glioblastomas, radiogenomic correlations are challenging, due to IDH mutations occurring in a small proportion (< 10%) of GBMs [2, 41, 43, 45, 47]. Corresponding to LGG characteristics, the two more useful GBM features for suggesting an IDH mutation are tumour location (frontal and/or insular) and a greater amount of nCET. However, in the case of a frontal lobe location, the association appears weaker than in LGG. Indeed, frontal location is moderately common in IDH^{wt} tumours, probably greater than for IDH^{mut} GBM in absolute terms [41–43]. Therefore, location can contribute to radiogenomic predictions with limited specificity.

No reliable WHO grade prediction is possible based on glioma enhancement properties for any glioma molecular subtype. IDH^{mut} tumours tend to demonstrate less enhancement than IDH^{wt} [22–24], and 1p19q^{code1} tumours may show ill-defined enhancement^{17, 19}, while ring-enhancement with central necrosis increases the likelihood of an IDH^{wt} glioma [11, 22, 26]. There are challenges with the use of nCET size comparisons; while a larger noncontrast-enhancing tumour proportion may indicate IDH^{mut} status [41], no size threshold is

applicable and most IDH^{wt} tumours exhibit nCET to some extent [43]. As such, it may be more appropriate to utilize “lack of nCET” to predict IDH^{wt} status [43].

A homogeneous, well-defined glioma is likely to be IDH^{mut}/1p19q^{intact}, while a heterogeneous, ill-defined tumour is likely IDH^{wt} or 1p19q^{code1}. Provided the glioma does not enhance [24], the presence of T2-FLAIR mismatch allows a confident designation as an IDH^{mut}/1p19q^{intact} astrocytoma [31, 38, 39]. With a published specificity of 100% in three different cohorts [31, 38, 39], this is the single most distinctive conventional MRI feature across both LGG and GBM, with moderate to substantial interobserver agreement. Several studies highlighted the value of indistinct non-enhancing lesion margins to identify IDH^{wt}, but this feature is problematic due to overlap with 1p19q^{code1}, and for reasons of subjectivity. In particular, the agreement reported for 2 observers by Park et al. ($\kappa = 0.766$) is discrepant from the much lower agreement ($\kappa = 0.374$, 95% CI 0.347–0.514) in multi-reader testing of the original VASARI research, which explicitly casted doubt on the reproducibility of this sign [27]. Calcifications in an untreated glioma suggest 1p19q^{code1} [16, 19, 35]; this should ideally be assessed on CT, as intratumoural susceptibility effects due to petechial haemorrhage are common in GBM, and have more recently been associated with IDH^{wt} LGG [49]. Several studies have highlighted an association between cyst formation and IDH^{mut} status [18, 22, 41], which underscores the importance of distinguishing this morphology from rim-enhancing necrosis during imaging assessments.

ADC values are generally highest in 1p19q^{intact}, lowest in IDH^{wt} and intermediate in 1p19q^{code1}, which is consistently reported in the literature. Furthermore, ADC is one of few metrics quantifiable on clinical MRI at the time of reporting, with substantial to near perfect interobserver agreement [18, 30]. It remains unclear whether minimum or mean ADC is most accurate, and whether normalizing ADC (e.g. to contralateral normal-appearing white matter) is beneficial. ADC values also appear higher in IDH^{mut} GBM, but there is less evidence for this and the results are not as compelling, with necrosis being a potential confounder of ADC quantification.

The systematic evaluation of genotyping literature was more challenging for LGG than in GBM, because numerous studies investigated either IDH or 1p19q status, or assessed both independently, with a three-group distinction according to the 2016 WHO criteria being less common. Consequently, it is not clear how accurate some particular visual features are for separating the three LGG subtypes in clinical practice, compared with examining a single molecular marker in a binary group distinction, due to a degree of overlap for most visually assessable MRI features across the three subtypes.

A number of strategies, including multivariate regression models, have been proposed to combine imaging features for glioma genotype predictions, but their method variability limits comparison. In general, features that are either specific

(to confidently predict a given molecular subtype) or sensitive (to exclude a subtype) are most suited to such an approach. Lasocki et al. suggested an algorithm combining the T2-FLAIR mismatch sign and the presence of calcifications, being predictive of 1p19q^{intact} and 1p19q^{codelet} tumours, respectively, with no overlap between the groups [35]. The main limitation of this algorithm was the sensitivity, as 38 of 59 in this cohort did not exhibit either feature [35]. Kanazawa et al. presented a scoring system for predicting 1p19q codeletion comprised of four features – calcification, indistinct tumour border on T1WI, paramagnetic susceptibility effect on T1WI and a cystic component on FLAIR – and found that the presence of at least three of the four features had a positive predictive value of 96% and specificity of 98% [19]. In the context of glioblastomas, the absence of either a frontal lobe location or at least 33% nCET has been reported as being strongly predictive of IDH^{wt} status [43].

A key finding of this analysis is that most studies performed no interobserver comparisons, so that human factors remain a concern for qualitative visual assessments in clinical practice. Thus, their diagnostic accuracy and variability remain to some extent uncertain, even when summarizing multiple studies.

Conclusions

A substantial body of literature exists on conventional MRI for glioma radiogenomic predictions, detailing findings in several thousand tumours. Despite heterogeneous methods, consistent result themes have emerged in this review with respect to tumour epicentres and signal characteristics, which indicate that conventional MRI is valuable for glioma genotyping, particularly in presumed LGG. However, due to sparse interobserver testing, the reproducibility of qualitative features remains an area of uncertainty.

Authors' contributions All authors contributed significantly to this research and have approved the final manuscript.

Data availability The data extraction table and QUADAS-2 table are provided as [Supplementary Material](#).

Funding information Arian Lasocki was supported by a Peter MacCallum Cancer Foundation Discovery Partner Fellowship. Stefanie Thust receives funding from the University College London/UCL Hospitals National Institute of Health Research Biomedical Research Centre.

Compliance with ethical standards

Conflict of interest None

Ethics approval The study was performed in accordance with the ethical standards as laid down in the 1964 Declaration of Helsinki and its later amendments. Formal ethics committee approval is not required for a study of this nature.

Informed consent Informed consent was obtained from all individual participants included in the study.

Code availability N/A

References

1. Louis DN, Perry A, Reifenberger G, von Deimling A, Figarella-Branger D, Cavenee WK, Ohgaki H, Wiestler OD, Kleihues P, Ellison DW (2016) The 2016 World Health Organization Classification of Tumors of the Central Nervous System: a summary. *Acta Neuropathol* 131(6):803–820. <https://doi.org/10.1007/s00401-016-1545-1>
2. Yan H, Parsons DW, Jin G, McLendon R, Rasheed BA, Yuan W, Kos I, Batinic-Haberle I, Jones S, Riggins GJ, Friedman H, Friedman A, Reardon D, Herndon J, Kinzler KW, Velculescu VE, Vogelstein B, Bigner DD (2009) IDH1 and IDH2 mutations in gliomas. *N Engl J Med* 360(8):765–773. <https://doi.org/10.1056/NEJMoa0808710>
3. Brat DJ, Aldape K, Colman H, Holland EC, Louis DN, Jenkins RB, Kleinschmidt-DeMasters BK, Perry A, Reifenberger G, Stupp R, von Deimling A, Weller M (2018) cIMPACT-NOW update 3: recommended diagnostic criteria for “Diffuse astrocytic glioma, IDH-wildtype, with molecular features of glioblastoma, WHO grade IV”. *Acta Neuropathol* 136(5):805–810. <https://doi.org/10.1007/s00401-018-1913-0>
4. Tesileanu CMS, Dirven L, Wijnenga MMJ, Koekkoek JAF, Vincent A, Dubbink HJ, Atmodimedjo PN, Kros JM, van Duinen SG, Smits M, Taphoorn MJB, French PJ, van den Bent MJ (2019) Survival of diffuse astrocytic glioma, IDH1/2-wildtype, with molecular features of glioblastoma, WHO grade IV: a confirmation of the cIMPACT-NOW criteria. *Neuro-Oncology* 22:515–523. <https://doi.org/10.1093/neuonc/noz200>
5. Ellingson BM, Bendszus M, Boxerman J, Barboriak D, Erickson BJ, Smits M, Nelson SJ, Gerstner E, Alexander B, Goldmacher G, Wick W, Vogelbaum M, Weller M, Galanis E, Kalpathy-Cramer J, Shankar L, Jacobs P, Pope WB, Yang D, Chung C, Knopp MV, Cha S, van den Bent MJ, Chang S, Yung WK, Cloughesy TF, Wen PY, Gilbert MR (2015) Consensus recommendations for a standardized Brain Tumor Imaging Protocol in clinical trials. *Neuro-Oncology* 17(9):1188–1198. <https://doi.org/10.1093/neuonc/nov095>
6. Thust SC, Heiland S, Falini A, Jager HR, Waldman AD, Sundgren PC, Godi C, Katsaros VK, Ramos A, Bargallo N, Vernooij MW, Youstry T, Bendszus M, Smits M (2018) Glioma imaging in Europe: A survey of 220 centres and recommendations for best clinical practice. *Eur Radiol* 28(8):3306–3317. <https://doi.org/10.1007/s00330-018-5314-5>
7. Smits M, van den Bent MJ (2017) Imaging Correlates of Adult Glioma Genotypes. *Radiology* 284(2):316–331. <https://doi.org/10.1148/radiol.2017151930>
8. McInnes MDF, Moher D, Thoms BD, McGrath TA, Bossuyt PM, Clifford T, Cohen JF, Deeks JJ, Gatsonis C, Hooft L, Hunt HA, Hyde CJ, Korevaar DA, Leeflang MMG, Macaskill P, Reitsma JB, Rodin R, Rutjes AWS, Salameh JP, Stevens A, Takwoingi Y, Tonelli M, Weeks L, Whiting P, Willis BH (2018) Preferred Reporting Items for a Systematic Review and Meta-analysis of Diagnostic Test Accuracy Studies: The PRISMA-DTA Statement. *JAMA* 319(4):388–396. <https://doi.org/10.1001/jama.2017.19163>
9. Whiting PF, Rutjes AW, Westwood ME, Mallett S, Deeks JJ, Reitsma JB, Leeflang MM, Sterne JA, Bossuyt PM (2011) QUADAS-2: a revised tool for the quality assessment of diagnostic

- accuracy studies. *Ann Intern Med* 155(8):529–536. <https://doi.org/10.7326/0003-4819-155-8-201110180-00009>
10. Qi S, Yu L, Li H, Ou Y, Qiu X, Ding Y, Han H, Zhang X (2014) Isocitrate dehydrogenase mutation is associated with tumor location and magnetic resonance imaging characteristics in astrocytic neoplasms. *Oncol Lett* 7(6):1895–1902. <https://doi.org/10.3892/ol.2014.2013>
 11. Sonoda Y, Shibahara I, Kawaguchi T, Saito R, Kanamori M, Watanabe M, Suzuki H, Kumabe T, Tominaga T (2015) Association between molecular alterations and tumor location and MRI characteristics in anaplastic gliomas. *Brain Tumor Pathol* 32(2):99–104. <https://doi.org/10.1007/s10014-014-0211-3>
 12. Wasserman JK, Nicholas G, Yaworski R, Wasserman AM, Woulfe JM, Jansen GH, Chakraborty S, Nguyen TB (2015) Radiological and pathological features associated with IDH1-R132H mutation status and early mortality in newly diagnosed anaplastic astrocytic tumours. *PLoS One* 10(4):e0123890. <https://doi.org/10.1371/journal.pone.0123890>
 13. Darlix A, Deverduin J, Menjot de Champfleury N, Castan F, Zouaoui S, Rigau V, Fabbro M, Yordanova Y, Le Bars E, Bauchet L, Goze C, Duffau H (2017) IDH mutation and 1p19q codeletion distinguish two radiological patterns of diffuse low-grade gliomas. *J Neuro-Oncol* 133(1):37–45. <https://doi.org/10.1007/s11060-017-2421-0>
 14. Xing Z, Yang X, She D, Lin Y, Zhang Y, Cao D (2017) Noninvasive assessment of IDH mutational status in World Health Organization grade II and III astrocytomas using DWI and DSC-PWI combined with conventional MR imaging. *AJNR Am J Neuroradiol* 38(6):1138–1144. <https://doi.org/10.3174/ajnr.A5171>
 15. Hyare H, Rice L, Thust S, Nachev P, Jha A, Milic M, Brandner S, Rees J (2019) Modelling MR and clinical features in grade II/III astrocytomas to predict IDH mutation status. *Eur J Radiol* 114:120–127. <https://doi.org/10.1016/j.ejrad.2019.03.003>
 16. Yamauchi T, Ohno M, Matsushita Y, Takahashi M, Miyakita Y, Kitagawa Y, Kondo E, Tsushita N, Satomi K, Yoshida A, Ichimura K, Narita Y (2018) Radiological characteristics based on isocitrate dehydrogenase mutations and 1p/19q codeletion in grade II and III gliomas. *Brain Tumor Pathol* 35(3):148–158. <https://doi.org/10.1007/s10014-018-0321-4>
 17. Delfanti RL, Piccioni DE, Handwerker J, Bahrami N, Krishnan A, Karunamuni R, Hattangadi-Gluth JA, Seibert TM, Srikant A, Jones KA, Snyder VS, Dale AM, White NS, McDonald CR, Farid N (2017) Imaging correlates for the 2016 update on WHO classification of grade II/III gliomas: implications for IDH, 1p/19q and ATRX status. *J Neuro-Oncol* 135(3):601–609. <https://doi.org/10.1007/s11060-017-2613-7>
 18. Villanueva-Meyer JE, Wood MD, Choi BS, Mabray MC, Butowski NA, Tihan T, Cha S (2018) MRI features and IDH mutational status of grade II diffuse gliomas: impact on diagnosis and prognosis. *AJR Am J Roentgenol* 210(3):621–628. <https://doi.org/10.2214/ajr.17.18457>
 19. Kanazawa T, Fujiwara H, Takahashi H, Nishiyama Y, Hirose Y, Tanaka S, Yoshida K, Sasaki H (2019) Imaging scoring systems for preoperative molecular diagnoses of lower-grade gliomas. *Neurosurg Rev* 42(2):433–441. <https://doi.org/10.1007/s10143-018-0981-x>
 20. Park YW, Han K, Ahn SS, Bae S, Choi YS, Chang JH, Kim SH, Kang SG, Lee SK (2018) Prediction of IDH1-mutation and 1p/19q-codeletion status using preoperative MR imaging phenotypes in lower grade gliomas. *AJNR Am J Neuroradiol* 39(1):37–42. <https://doi.org/10.3174/ajnr.A5421>
 21. Compes P, Tabouret E, Etchevery A, Colin C, Appay R, Cordier N, Mosser J, Chinot O, Delingette H, Girard N, Dufour H, Metellus P, Figarella-Branger D (2019) Neuro-radiological characteristics of adult diffuse grade II and III insular gliomas classified according to WHO 2016. *J Neuro-Oncol* 142(3):511–520. <https://doi.org/10.1007/s11060-019-03122-1>
 22. Wu CC, Jain R, Radmanesh A, Poisson LM, Guo WY, Zagzag D, Snuderl M, Placantonakis DG, Golfinos J, Chi AS (2018) Predicting genotype and survival in glioma using standard clinical MR imaging apparent diffusion coefficient images: a pilot study from The Cancer Genome Atlas. *AJNR Am J Neuroradiol* 39(10):1814–1820. <https://doi.org/10.3174/ajnr.A5794>
 23. Wang YY, Wang K, Li SW, Wang JF, Ma J, Jiang T, Dai JP (2015) Patterns of tumor contrast enhancement predict the prognosis of anaplastic gliomas with IDH1 mutation. *AJNR Am J Neuroradiol* 36(11):2023–2029. <https://doi.org/10.3174/ajnr.A4407>
 24. Juratli TA, Tummala SS, Riedl A, Daubner D, Hennig S, Penson T, Zolal A, Thiede C, Schackert G, Krex D, Miller JJ, Cahill DP (2019) Radiographic assessment of contrast enhancement and T2/FLAIR mismatch sign in lower grade gliomas: correlation with molecular groups. *J Neuro-Oncol* 141(2):327–335. <https://doi.org/10.1007/s11060-018-03034-6>
 25. Su CQ, Lu SS, Zhou MD, Shen H, Shi HB, Hong XN (2019) Combined texture analysis of diffusion-weighted imaging with conventional MRI for non-invasive assessment of IDH1 mutation in anaplastic gliomas. *Clin Radiol* 74(2):154–160. <https://doi.org/10.1016/j.crad.2018.10.002>
 26. Reyes-Botero G, Dehais C, Idbaih A, Martin-Duverneuil N, Lahutte M, Carpentier C, Letouze E, Chinot O, Loiseau H, Honnorat J, Ramirez C, Moyal E, Figarella-Branger D, Ducray F (2014) Contrast enhancement in 1p/19q-codeleted anaplastic oligodendrogliomas is associated with 9p loss, genomic instability, and angiogenic gene expression. *Neuro-Oncology* 16(5):662–670. <https://doi.org/10.1093/neuonc/not235>
 27. Wiki for the VASARI feature set. The National Cancer Institute website. 2015. Available at: <https://wiki.cancerimagingarchive.net/display/Public/VASARI+Research+Project>. Accessed Dec 2019
 28. Zhou H, Vallieres M, Bai HX, Su C, Tang H, Oldridge D, Zhang Z, Xiao B, Liao W, Tao Y, Zhou J, Zhang P, Yang L (2017) MRI features predict survival and molecular markers in diffuse lower-grade gliomas. *Neuro-Oncology* 19(6):862–870. <https://doi.org/10.1093/neuonc/nw256>
 29. Liu T, Cheng G, Kang X, Xi Y, Zhu Y, Wang K, Sun C, Ye J, Li P, Yin H (2018) Noninvasively evaluating the grading and IDH1 mutation status of diffuse gliomas by three-dimensional pseudo-continuous arterial spin labeling and diffusion-weighted imaging. *Neuroradiology* 60(7):693–702. <https://doi.org/10.1007/s00234-018-2021-5>
 30. Thust SC, Hassanein S, Bisdas S, Rees JH, Hyare H, Maynard JA, Brandner S, Tur C, Jager HR, Yousry TA, Mancini L (2018) Apparent diffusion coefficient for molecular subtyping of non-gadolinium-enhancing WHO grade II/III glioma: volumetric segmentation versus two-dimensional region of interest analysis. *Eur Radiol* 28(9):3779–3788. <https://doi.org/10.1007/s00330-018-5351-0>
 31. Batchala PP, Muttikkal TJE, Donahue JH, Patrie JT, Schiff D, Fadul CE, Mrachek EK, Lopes MB, Jain R, Patel SH (2019) Neuroimaging-based classification algorithm for predicting 1p/19q-codeletion status in IDH-mutant lower grade gliomas. *AJNR Am J Neuroradiol* 40(3):426–432. <https://doi.org/10.3174/ajnr.A5957>
 32. Johnson DR, Diehn FE, Giannini C, Jenkins RB, Jenkins SM, Parney IF, Kaufmann TJ (2017) Genetically defined oligodendroglioma is characterized by indistinct tumor borders at MRI. *AJNR Am J Neuroradiol* 38(4):678–684. <https://doi.org/10.3174/ajnr.A5070>
 33. Kim JW, Park CK, Park SH, Kim YH, Han JH, Kim CY, Sohn CH, Chang KH, Jung HW (2011) Relationship between radiological characteristics and combined 1p and 19q deletion in World Health Organization grade III oligodendroglial tumours. *J Neurol*

- Neurosurg Psychiatry 82(2):224–227. <https://doi.org/10.1136/jnnp.2009.178806>
34. Sherman JH, Prevedello DM, Shah L, Raghavan P, Pouratian N, Starke RM, Lopes MB, Shaffrey ME, Schiff D (2010) MR imaging characteristics of oligodendroglial tumors with assessment of 1p/19q deletion status. *Acta Neurochir* 152(11):1827–1834. <https://doi.org/10.1007/s00701-010-0743-1>
 35. Lasocki A, Gaillard F, Gorelik A, Gonzales M (2018) MRI features can predict 1p/19q status in intracranial gliomas. *AJNR Am J Neuroradiol* 39(4):687–692. <https://doi.org/10.3174/ajnr.A5572>
 36. Xiong J, Tan W, Wen J, Pan J, Wang Y, Zhang J, Geng D (2016) Combination of diffusion tensor imaging and conventional MRI correlates with isocitrate dehydrogenase 1/2 mutations but not 1p/19q genotyping in oligodendroglial tumours. *Eur Radiol* 26(6):1705–1715. <https://doi.org/10.1007/s00330-015-4025-4>
 37. Peng X, Yishuang C, Kaizhou Z, Xiao L, Ma C (2019) Conventional magnetic resonance features for predicting 1p19q codeletion status of World Health Organization grade II and III diffuse gliomas. *J Comput Assist Tomogr* 43(2):269–276. <https://doi.org/10.1097/rct.0000000000000816>
 38. Patel SH, Poisson LM, Brat DJ, Zhou Y, Cooper L, Snuderl M, Thomas C, Franceschi AM, Griffith B, Flanders AE, Golfinos JG, Chi AS, Jain R (2017) T2-FLAIR mismatch, an imaging biomarker for IDH and 1p/19q status in lower-grade gliomas: a TCGA/TClA project. *Clin Cancer Res* 23(20):6078–6085. <https://doi.org/10.1158/1078-0432.Ccr-17-0560>
 39. Broen MPG, Smits M, Wijnenga MMJ, Dubbink HJ, Anten M, Schijns O, Beckervordersandforth J, Postma AA, van den Bent MJ (2018) The T2-FLAIR mismatch sign as an imaging marker for non-enhancing IDH-mutant, 1p/19q-intact lower-grade glioma: a validation study. *Neuro-Oncology* 20(10):1393–1399. <https://doi.org/10.1093/neuonc/noy048>
 40. Cui Y, Ma L, Chen X, Zhang Z, Jiang H, Lin S (2014) Lower apparent diffusion coefficients indicate distinct prognosis in low-grade and high-grade glioma. *J Neuro-Oncol* 119(2):377–385. <https://doi.org/10.1007/s11060-014-1490-6>
 41. Carrillo JA, Lai A, Nghiemphu PL, Kim HJ, Phillips HS, Kharbanda S, Moftakhar P, Lalaezari S, Yong W, Ellingson BM, Cloughesy TF, Pope WB (2012) Relationship between tumor enhancement, edema, IDH1 mutational status, MGMT promoter methylation, and survival in glioblastoma. *AJNR Am J Neuroradiol* 33(7):1349–1355. <https://doi.org/10.3174/ajnr.A2950>
 42. Xing Z, Zhang H, She D, Lin Y, Zhou X, Zeng Z, Cao D (2019) IDH genotypes differentiation in glioblastomas using DWI and DSC-PWI in the enhancing and peri-enhancing region. *Acta Radiol*:284185119842288. <https://doi.org/10.1177/0284185119842288>
 43. Lasocki A, Tsui A, Gaillard F, Tacey M, Drummond K, Stuckey S (2017) Reliability of noncontrast-enhancing tumor as a biomarker of IDH1 mutation status in glioblastoma. *J Clin Neurosci* 39:170–175. <https://doi.org/10.1016/j.jocn.2017.01.007>
 44. Hong EK, Choi SH, Shin DJ, Jo SW, Yoo RE, Kang KM, Yun TJ, Kim JH, Sohn CH, Park SH, Won JK, Kim TM, Park CK, Kim IH, Lee ST (2018) Radiogenomics correlation between MR imaging features and major genetic profiles in glioblastoma. *Eur Radiol* 28(10):4350–4361. <https://doi.org/10.1007/s00330-018-5400-8>
 45. Hata N, Hatae R, Yoshimoto K, Murata H, Kuga D, Akagi Y, Sangatsuda Y, Suzuki SO, Iwaki T, Mizoguchi M, Iihara K (2017) Insular primary glioblastomas with IDH mutations: Clinical and biological specificities. *Neuropathology* 37(3):200–206. <https://doi.org/10.1111/neup.12362>
 46. Yamashita K, Hiwatashi A, Togao O, Kikuchi K, Hatae R, Yoshimoto K, Mizoguchi M, Suzuki SO, Yoshiura T, Honda H (2016) MR Imaging-based analysis of glioblastoma multiforme: estimation of IDH1 mutation status. *AJNR Am J Neuroradiol* 37(1):58–65. <https://doi.org/10.3174/ajnr.A4491>
 47. Wang K, Wang Y, Fan X, Wang J, Li G, Ma J, Ma J, Jiang T, Dai J (2016) Radiological features combined with IDH1 status for predicting the survival outcome of glioblastoma patients. *Neuro-oncology* 18(4):589–597. <https://doi.org/10.1093/neuonc/nov239>
 48. Lasocki A, Gaillard F, Tacey M, Drummond K, Stuckey S (2018) Morphologic patterns of noncontrast-enhancing tumor in glioblastoma correlate with IDH1 mutation status and patient survival. *J Clin Neurosci* 47:168–173. <https://doi.org/10.1016/j.jocn.2017.09.007>
 49. Kong LW, Chen J, Zhao H, Yao K, Fang SY, Wang Z, Wang YY, Li SW (2019) Intratumoral susceptibility signals reflect biomarker status in gliomas. *Sci Rep* 9(1):17080. <https://doi.org/10.1038/s41598-019-53629-w>

Publisher's note Springer Nature remains neutral with regard to jurisdictional claims in published maps and institutional affiliations.